CANADIAN JOURNAL OF EXPLORATION GEOPHYSICS
VOL. 29, NO. 1 (JUNE 1993), P. 227-235

DISPLAYING SHEAR-WAVE SPLITTING IN CROSS-HOLE SURVEYS FOR MATERIALS WITH COMBINATIONS OF EDA AND PTL ANISOTROPIES

BRIAN BAPTIE[1], STUART CRAMPIN[1] AND ENRU LIU[2]

ABSTRACT

This paper addresses two current developments: the increasing number of cross-hole surveys and horizontal wells and the recognition of combinations of matrix anisotropy and the anisotropy due to vertical fractures in sedimentary basins. The dip of raypaths in cross-hole surveys and other subsurface surveys is significantly different from the near-vertical raypaths in reflection surveys and vertical seismic profiles. Consequently, polar projections are no longer appropriate for displaying the parameters of shear-wave splitting in cross-hole surveys. Here we present shear-wave polarizations and time delays between faster and slower split shear-wave arrivals in more convenient Plate Carée (equal-area cylindrical) projections for a range of combinations of EDA and PTL anisotropy (crack anisotropy and matrix anisotropy, respectively) common in sedimentary basins. The combination of these two types of hexagonal anisotropic symmetry, with perpendicular axes, leads to orthorhombic symmetry with three mutually perpendicular symmetry planes. In such orthorhombic systems, shear waves display anomalous behaviour in directions of propagation near point singularities, where the polarizations and amplitudes of rays of shear waves may fluctuate rapidly for small changes in direction. The three-dimensional variations in polarizations, time delays and positions of point singularities can be used for the interpretation of multicomponent shear-wave data sets in cross-hole and other subsurface surveys.

INTRODUCTION

Shear-wave splitting is commonly observed in sedimentary basins in three-component shear-wave reflection surveys, vertical seismic profiles (VSPs) and cross-hole surveys (CHSs) [see recent review by Crampin and Love11 (1991)]. Such behaviour is characteristic of shear-wave propagation in at least the upper half of the crust and is diagnostic of some form of seismic anisotropy along the raypath (Crampin, 1985a). Typically, the polarization of the shear waves for nearly vertical propagation is scattered about the direction of maximum horizontal stress (Crampin, 1987; Crampin and Lovell, 1991). The polarization of the shear-wave splitting along nearly vertical raypaths has been used to obtain the orientation of subsurface fractures (Mueller, 1991, 1992) and the delay between the split shear waves has been correlated with the rate of hydrocarbon production (Cliet et al., 199 1; Lewis et al., 1991; Li et al., 1993). As a result, monitoring the distinctive behaviour of shear waves appears to have direct applications to reservoir characterization and optimization of production.

Bush and Crampin (1987, 199 1) in the Paris Basin, Yardley and Crampin (1993) in Texas, Slater et al. (1993) in the Caucasus and others, have shown that the anisotropy of sedimentary basins may be the result of combinations of azimuthal *anisotropy* and transverse isotropy with a vertical axis of symmetry [azimuthal *isotropy*, in the terminology of Crampin (1989)]. The azimuthal anisotropy appears to be caused by cracks, microcracks and preferentially oriented pore space known as *extensive-dilatancy anisotropy* or EDA (Crampin, 1987, 1993a; Crampin and Lovell, 199 1). Azimuthal isotropy is a matrix anisotropy, characterized by *P*- and *S*-waves travelling faster in horizontal than in vertical directions. It can be caused either by aligned grains such as shales (Kaarsberg, 1968; Robertson and Corrigan, 1983) or by finely layered horizontal bedding (Krey and Helbig, 1956; Levin, 1979, 1980) which can be conveniently modelled by repeated (P)eriodic sequences of (T)hin (L)ayers (Postma, 1955), which we shall call *PTL anisotropy* (Crampin, 1989). Since aligned grains and bedding have similar seismic properties, we shall use the term PTL anisotropy to refer to both types of matrix anisotropy.

Typically, PTL anisotropy and EDA anisotropy have orthogonal symmetry axes (vertical for PTL and horizontal for EDA). The combination of PTL and EDA anisotropy leads to orthorhombic symmetry (Wild and Crampin, 199 1), which we shall call (C)racked (L)ayer (A)nisotropy or *CLA anisotropy*. The polar projections of, for example, Wild and Crampin (199 1) and many others are appropriate for the nearly vertical raypaths in reflection surveys and VSPs. However, with the increasing use of more horizontal raypaths in

'Edinburgh Anisotropy Project, British Geological Survey, Murchison House, West Mains Road, Edinburgh EH9 3LA; also, Department of Geology and Geophysics, University of Edinburgh, Grant Institute, West Mains Road, Edinburgh EH9 3JW

'British Geological Survey, Murchison House, West Mains Road, Edinburgh EH9 3LA

This research was supported by the Sponsors of the Edinburgh Anisotropy Project and the Natural Environment Research Council and is published with the approval of the Director of the British Geological Survey (NERC).

CHSs and between horizontal wells, polar plots are no longer adequate. (Equatorial regions are heavily distorted in polar plots centred on the North Pole.)

This paper demonstrates the behaviour of shear-wave splitting for a range of combinations of EDA and PTL anisotropies in Plate Carée (equal-area cylindrical) projections (following Liu et al., 1989) to aid the interpretation of shear waves from CHSs. Holmes et al. (1993), in this issue, has used such projections to display the polarizations of microcracks in a controlled-source shear-wave survey over a wide range of azimuths and angles of incidence in the Underground Research Laboratory at Pinawa, Manitoba, of the Atomic Energy of Canada Ltd.

Shear-wave Propagation in Anisotropic Solids

The behaviour of shear waves in anisotropic solids is fundamentally different from their behaviour in isotropic media, although the differences may be subtle and easily overlooked. Two shear waves propagate in every direction of phase velocity with the faster, *qS*1-, and slower, *qS*2-waves, having mutually orthogonal polarizations. The differences in velocity and polarization between the two waves leads to the phenomena of shear-wave splitting (Crampin, 1978, 1981) which introduces phase and amplitude differences into the different components of motion. The polarizations and delays measured from split shear waves may be used to estimate orientations and percentages of anisotropy and hence, the orientations and densities of subsurface cracks and fractures.

A further complication is that traveltimes estimated from field observations are measured along seismic rays propagating at the group velocity and seldom allow phase velocity to be estimated directly. In anisotropic solids, where the group velocity diverges from the phase velocity both in magnitude and direction, the polarizations of the two shear waves are no longer mutually orthogonal for propagation along seismic rays at the group velocity except in certain symmetry directions (Crampin, 198 1, 1989).

Consequently, the variation of shear-wave velocities in anisotropic solids can be described by two surfaces referring to phase and group velocity. The phase-velocity surfaces are analytically continuous and must touch in at least two directions (usually many more) called shear-wave singularities (Crampin and Yedlin, 1981). There are three distinct types of singularity: line, kiss and point singularities. Sections of phase-velocity surfaces near point singularities, the commonest type of singularity, usually display high curvature, so that shear-wave polarizations may vary rapidly for small differences in raypath direction. This causes shear waves, propagating at group velocity, to show anomalies in polarizations and amplitudes as well as various cuspoidal features (Crampin, 1991). It was the behaviour of shear-wave polarizations in multioffset VSPs in the Paris Basin that allowed Bush and Crampin (1987, 199 1) to recognize for the first time the presence of combinations of EDA and PTL anisotropy in sedimentary basins.

Wild and Crampin (199 1) show that combinations of EDA and PTL anisotropies have, necessarily, many directions of point singularities, where rays of shear waves have anomalous particle motion. The directions of these singularities are dependent on the types and relative proportions of EDA and PTL anisotropy in the rock mass. Since the faster split shear wave may not be polarized parallel to the crack strike for near vertical raypaths, it is necessary to understand the behaviour of combinations of EDA and PTL anisotropy in order to identify the orientations of subsurface fracturing.

Formulations for EDA and PTL

The five independent elastic constants of a PTL solid may be derived from the elastic properties and the ratio of thicknesses of repeated sequences of isotropic layers, by the formulations of Postma (I 955). These are valid for layer thicknesses of less than about half a seismic wavelength. The resultant structure has hexagonal anisotropic symmetry, with the axis of symmetry normal to the layering assumed to be vertical. In this paper, varying amounts of PTL anisotropy are expressed as the percentage of differential shear-wave velocity anisotropy (Crampin, 1989). The elastic constants for the PTL materials used in this paper are given in Table 1. These are derived from layer velocities typical of those observed in sedimentary basins.

Table 1. Elastic constants of PTL anisotropy, in 10^9Pa. Density = 2.6 g/cm^3.

	% anisotropy	$c_{1111} = c_{2222}$	c_{3333}	c_{1122}	$c_{3311} = c_{2233}$	$c_{2323} = c_{1313}$
PTL1	2%	41.378	39.690	15.808	15.186	12.418
PTL2	12%	32.272	24.835	11.907	9.509	7.949
PTL3	22%	28.576	17.369	10.156	6.644	5.631

The other principal form of seismic anisotropy, recognized by azimuthal variations in shear-wave behaviour, can be modelled by distributions of stress-aligned, fluid-filled microcracks and orientated pore space (Crampin, 1984, 1985b), known as extensive-dilatancy anisotropy or EDA. Such EDA cracks are aligned normal to the minimum compressional stress and, since this direction is usually horizontal below near-surface stress anomalies (Crampin, 1990), the cracks are typically aligned vertical, striking parallel to the maximum horizontal compressional stress.

EDA cracks are calculated with the formulations of Hudson (1980, 198 1) and incorporated into PTL anisotropy using the formulations of Hudson (1986) for the scattering of seismic waves by distributions of aligned cracks in anisotropic solids. Crack density, E, and aspect ratio, γ, are defined as $\varepsilon = Na^3/v$ and $\gamma = d/a$, respectively, where N is the number of cracks of radius a and half thickness d in volume v. Crack dimensions are assumed to be small with respect to seismic wavelength (Crampin, 1993b) and the approximations are thought to be valid for $\varepsilon < 0.1$ (Crampin 1984) and $\gamma < 0.3$ (Douma and Crampin, 1990). In this paper, we use

crack densities of $\varepsilon = 0.01$ and $\varepsilon = 0.05$ and aspect ratios of $\gamma = 0.001$ and $\gamma = 0.05$. EDA cracks also have hexagonal symmetry with, typically, a horizontal axis of symmetry.

The elastic constants for each combination are used to calculate polarizations and delays using the Kelvin-Christoffel equations, which give the components of the elastic tensor matrix in terms of the elastic constants and the phase velocity direction cosines. The eigenvalues and eigenvectors of the matrix give velocities and polarizations, respectively, of the three body waves. Group velocities are calculated and plotted for a grid of phase-velocity directions. As phase and group velocities are not coincident in anisotropic solids, this procedure leads to some distortion. This distortion is negligible for PTL of 2% but will be more significant for PTL anisotropies of 12% and 22%, although the general patterns of behaviour are preserved.

Shear-wave Splitting in Plate Carée Projections

The behaviour of shear-wave splitting in Plate Caree projections is demonstrated in Figure 1 for (a) PTL, (b) EDA and (c) CLA anisotropy, following Liu et al. (1989). The polarizations of the leading split shear wave, projected onto the horizontal radial/transverse (R-T) plane and the vertical/transverse (V-T) plane, are shown for a full range of raypaths, covering 360" of azimuth, and dips from +90° for downward propagation to -90" for upwards propagation. This represents the polarizations of shear waves radiating from a point source, as measured by horizontal instruments (R-T plane) and vertical-transverse instruments (V-T plane), on the walls of a cylinder enclosing the source. The cylinder has then been opened out (mapped) to give a conventional Cartesian (Plate Caree) map projection. Contoured normalized time delays between the fast and slow split shear waves are shown and north-south sections of the contours at five specified azimuths.

Figure la shows the behaviour of shear waves in a purely PTL material, PTL2, having 12% differential shear-wave velocity anisotropy (constants listed in Table 1). Figure 1 b shows the pattern of polarizations and delays for shear waves propagating through parallel vertical water-filled EDA cracks, striking east-west, with a crack density of $\varepsilon = 0.05$ and $\gamma = 0.05$, representing 5% differential shear-wave anisotropy, in an isotropic matrix ($a = 3.5$, $\beta = 2.02$ km/s, $\rho = 2.2$ g/cm^3). The effect of inserting the EDA cracks of Figure lb into the matrix with PTL anisotropy of Figure la leading to CLA anisotropy is shown in Figure lc.

The purely PTL anisotropy in Figure la shows a distinctive band of transverse polarizations of the leading split shear wave, for directions of propagation between about ±30° of the horizontal, representing SH-wave motion. Outside this band, shear waves are polarized in the sagittal plane, representing SV-motion. The 90" change in polarizations marks the direction of a line singularity (indicated by arrowheads), characteristic of hexagonal symmetry (Crampin, 1989). There are also kiss singularities, indicated by dots, in the directions of the symmetry axes – the North and South poles of Figure la. Time delays are largest for horizontal directions.

The projection of purely EDA anisotropy in Figure 1 b also shows distinctive patterns of behaviour. There is a band of nearly parallel polarizations for azimuths close to the crack strike in both R-T and V-T projections, where the time delays have their largest values. Line singularities (indicated by arrowheads), where polarizations of the leading shear wave change by an average of 90°, are also present, but with an orthogonal orientation to those for PTL anisotropy. Two kiss-singularities are marked with dots. The patterns of polarizations and delays, produced by EDA anisotropy in Plate Caree projections, lack any strongly diagnostic features such as seen in polar projections, where the polarization of shear waves along one near-vertical raypath can demonstrate the strike of the EDA cracks. This means that observations from a large number of directions of dip and azimuth are required to identify the characteristics of EDA anisotropy in CHSs (Liu et al., 1989).

The combined PTL and EDA anisotropies in Figure lc yield CLA anisotropy with patterns of polarizations and delays displaying orthorhombic symmetry. The line singularities of Figures la and 1 b have pulled apart and point singularities have appeared on the traces of these pull-apart remnants of line singularities (Crampin, 1989). These point singularities, in directions approximately indicated by circles, are places where the phase velocity surfaces touch at the vertices of convex and concave cones. The polarizations and time delays along seismic rays propagating at the group velocity may be much more complicated, with complex cuspoidal lids, fins and ridges on the surface of the group velocity surfaces (Crampin, 1991). These features are irregular in outline and frequently do not have clearly defined centres. Consequently, the positions of the circles merely indicates the approximate centre of the anomaly. In particular, polarizations and time delays may vary rapidly near point singularities and may lead to anomalous shear-wave amplitudes, polarizations and time delays, such as those observed by Bush and Crampin (1991).

Combinations of EDA and PTL Anisotropy in Plate Carée Projections

The pattern of shear-wave behaviour for a range of directions in rocks with CLA anisotropy varies significantly with the relative amounts of PTL anisotropy and the relative crack densities and aspect ratios of the distribution of parallel vertical cracks. Figures 2, 3 and 4 show Plate Caree projections of delays and polarizations produced by EDA cracks introduced into three different PTL solids. The PTL materials: PTL1, PTL2 and PTL3, respectively, have anisotropies with differential shear-wave velocities of 2%, 12% and 22%. The EDA cracks are specified by crack densities of $\varepsilon = 0.01$ and 0.05 (giving differential shear-wave velocity anisotropies due to the aligned cracks of approximately 1% and 5%) and by aspect ratios of y = 0.00 1 and 0.05. The figures are similar in format and notation to Figure 1. Note that there is inversion symmetry about a point source for all anisotropic variations in uniform homogeneous solids.

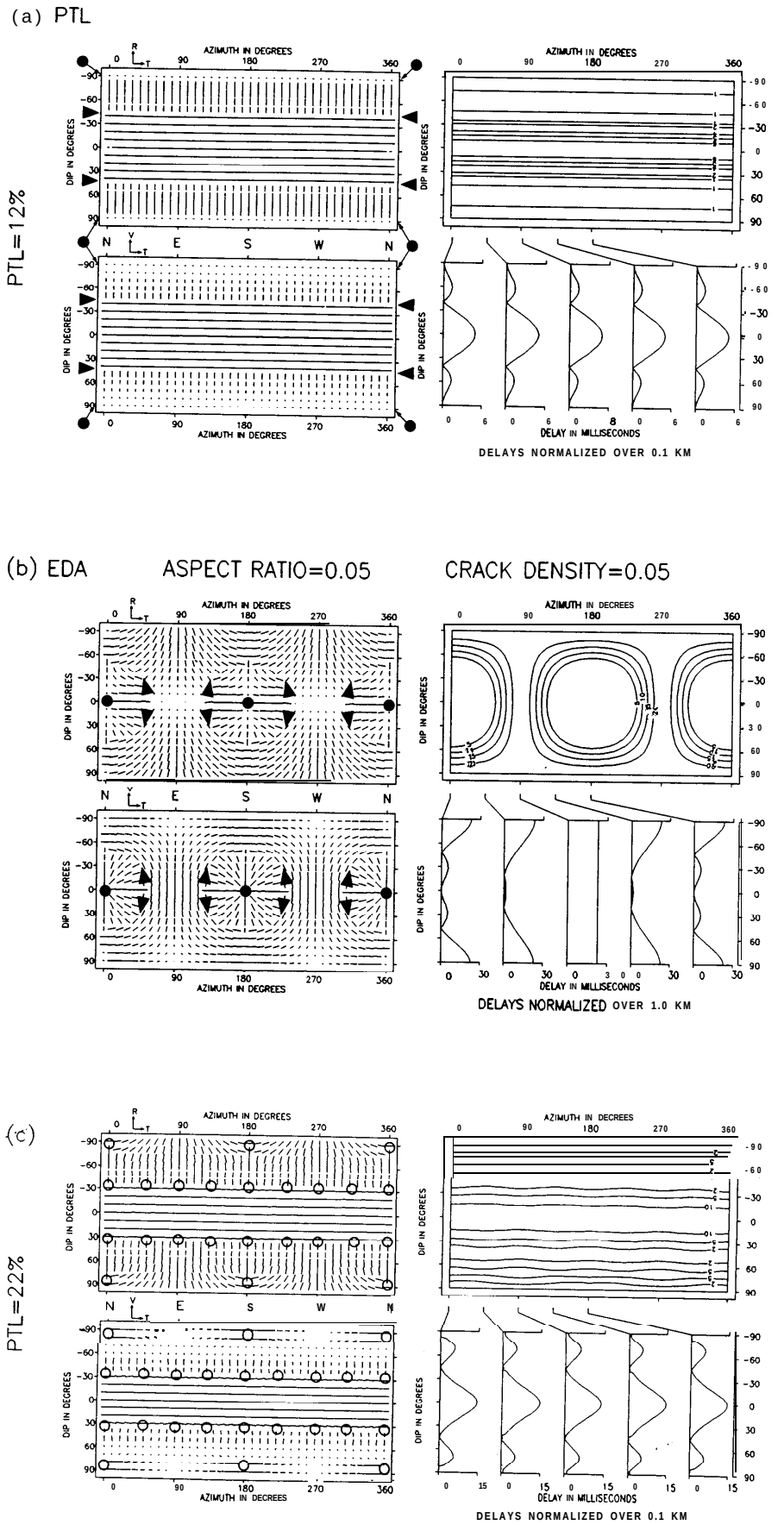

Fig. 1. Plate Carée equal-area cylindrical projections of the polarizations and time delays of split shear waves propagating along rays at the group velocity through: **(a)** PTL anisotropy with 12% differential shear-wave anisotropy; **(b)** EDA anisotropy of parallel vertical cracks striking east-west with crack density of $\varepsilon = 0.05$ and aspect ratio $\gamma = 0.05$; and (c) CLA anisotropy combining material in (a) with the cracks in (b). The four sections of each figure are: polarizations of leading split shear waves projected onto, top left, (R)adial/(T)ransverse (R-T) planes and, bottom left, (V)ertical/(T)ransverse (V-T) planes; and, top right, contours of the time delays in ms normalized over 100 m and, bottom right, north-south sections of contoured time delays at indicated azimuths. The polarizations show projections of a fixed-length vector on to the appropriate R-T and V-T planes. Arrows indicate directions of line singularities, solid circles indicate directions of kiss singularities and open circles indicate approximate directions of point singularities. Azimuths are measured from North through East.

The directions of point singularities in these orthorhombic symmetries are sensitive to changes in the relative parameters of the anisotropies making up the CLA anisotropy. Their directions may be used as a benchmark to describe the differences between each projection.

Variations in PTL anisotropy

Figure 2 shows the effects of variations in PTL anisotropy. Combinations of three PTL solids, PTL1, PTL2 and PTL3, with differential shear-wave anisotropies of 2%, 12% and 22%, respectively, are shown pervaded by thin cracks with crack density $\varepsilon = 0.01$ and aspect ratio $\gamma = 0.001$. For the strong PTL anisotropy of 22% for PTL3 in Figure 2c, the broad band of transverse polarizations of pure PTL (Figure la) is still present, but the line singularities at the edge of the broad band have each been replaced by eight nearly coplanar point singularities (Crampin, 1989). The kiss singularity, which exists for vertical directions of propagation in pure PTL anisotropy with hexagonal symmetry (Figure la), has divided into two point singularities which have moved towards the horizontal plane at azimuths of 0" and 180° (the 360" azimuth is a repeat of the 0" azimuth).

In contrast, in Figure 2a (PTLI), where the PTL anisotropy is comparable to the crack anisotropy, the singularities which in Figure 2c are close to the directions of line singularity of the pure PTL anisotropy (Figure la) have now moved closer to the line singularity in the pure EDA anisotropy in Figure lb. Again, the line singularity has been replaced by eight point singularities. The three-dimensional distribution of the singularities corresponding to the projection shown in Figure 2a is approximately equivalent to the distribution shown in Figure 2c, rotated by 90" about a horizontal E-W axis (azimuth 90°).

For the intermediate PTL anisotropy of 12% for PTL2 in Figure 2b, the point singularities are dispersed in directions between the almost planar line singularities in PTL and the almost planar singularities of EDA anisotropy (which are perpendicular because of the orthogonal symmetry axes). As the ratio of relative PTL and EDA anisotropies changes, the point singularity derived from the kiss singularity moves towards the pull-apart remnant of the line singularity and displaces a point singularity which moves towards the centre of the orthogonal pull-apart remnant line singularity.

The other effect of decreasing the amount of PTL, for a fixed crack anisotropy, is to decrease the time delays between the first and second split shear waves. For PTL3 (22%) the maximum delay is around 15 ms (normalized over 0.1 km). For PTL2 (12%) the maximum delay is about half this value, while for PTL1 (2%) the maximum delay has decreased to about 10 ms. Note that in Figure 2a for convenience the delays have been normalized over 1 km, whereas in Figures 2b and 2c they are normalized over 100 m.

Variations in EDA crack density

Figures 2 and 3 show the same PTL anisotropies for two different crack densities, $\varepsilon = 0.01$ and 0.05, for a constant aspect ratio of $\gamma = 0.001$. It can be seen that increasing crack density produces similar effects as reducing the percentage of PTL anisotropy, since the directions of the singularities are dependent on the ratio of EDA to PTL anisotropies. The point singularities move away from directions centred around one symmetry axis to directions centred around the other symmetry axis. Examining Figures 2a and 3a we can see that as the crack anisotropy exceeds that due to the PTL this shift in the symmetry axes becomes more complete. With increasing crack density, the band of parallel polarizations parallel to the crack strike becomes much more pronounced. Delays increase with crack density increases in each of the three PTL anisotropies.

Variations in EDA crack aspect ratio

The effect of varying aspect ratio can be seen by comparing Figures 3 and 4 which have the same PTL anisotropies pervaded by cracks of the same crack density ($\varepsilon = 0.05$) with two different aspect ratios, $\gamma = 0.001$ and 0.05, respectively. Changing aspect ratio makes comparatively little difference to the directions of the singularities for PTL anisotropies of 12% and 22%. However, the point singularities away from the equator tend to cluster together with increasing aspect ratio at about 45" from the horizontal direction, which is most marked for PTL of 2%.

Discussion

Observations in CHSs are usually strictly confined to raypaths in a few vertical sections within about 45" of the horizontal. It is clear from examining any of Figures l-4 that such raypaths in a limited number of vertical sections will probably not yield enough diagnostic information to identify PTL and EDA anisotropies and orientations. This is a different situation from polar projections of vertical motion, when a few nearly vertical rays of shear waves can lead to estimates of crack strike and stress orientation (Crampin and Lovell, 1991).

However, cross-hole surveys do present the opportunity to examine shear waves at higher resolution, with the advantages of higher frequencies and raypaths where most of the path is in the zone of interest, as well as avoiding the sometimes severe interactions of the shear waves with the free surface (Evans, 1984; Booth and Crampin, 1985). The greater resolution offered by CHSs should allow a more detailed evaluation of the anisotropy present in a rock mass by analyzing shear-wave splitting.

Difficulties arise if the cross-hole surveys include boundaries with significant impedance contrasts. The polarizations of shear waves crossing such boundaries at oblique angles suffer from the effects of the internal shear-wave window (Liu and Crampin, 1990). In addition, various interface waves may be guided or trapped by the boundary, so that in some cases the dominant energy of the CHS-seismograms will be in guided waves not body waves (Liu et al., 1991).

Changes in the properties of shear-wave splitting for the varying amounts of EDA and PTL anisotropy demonstrates

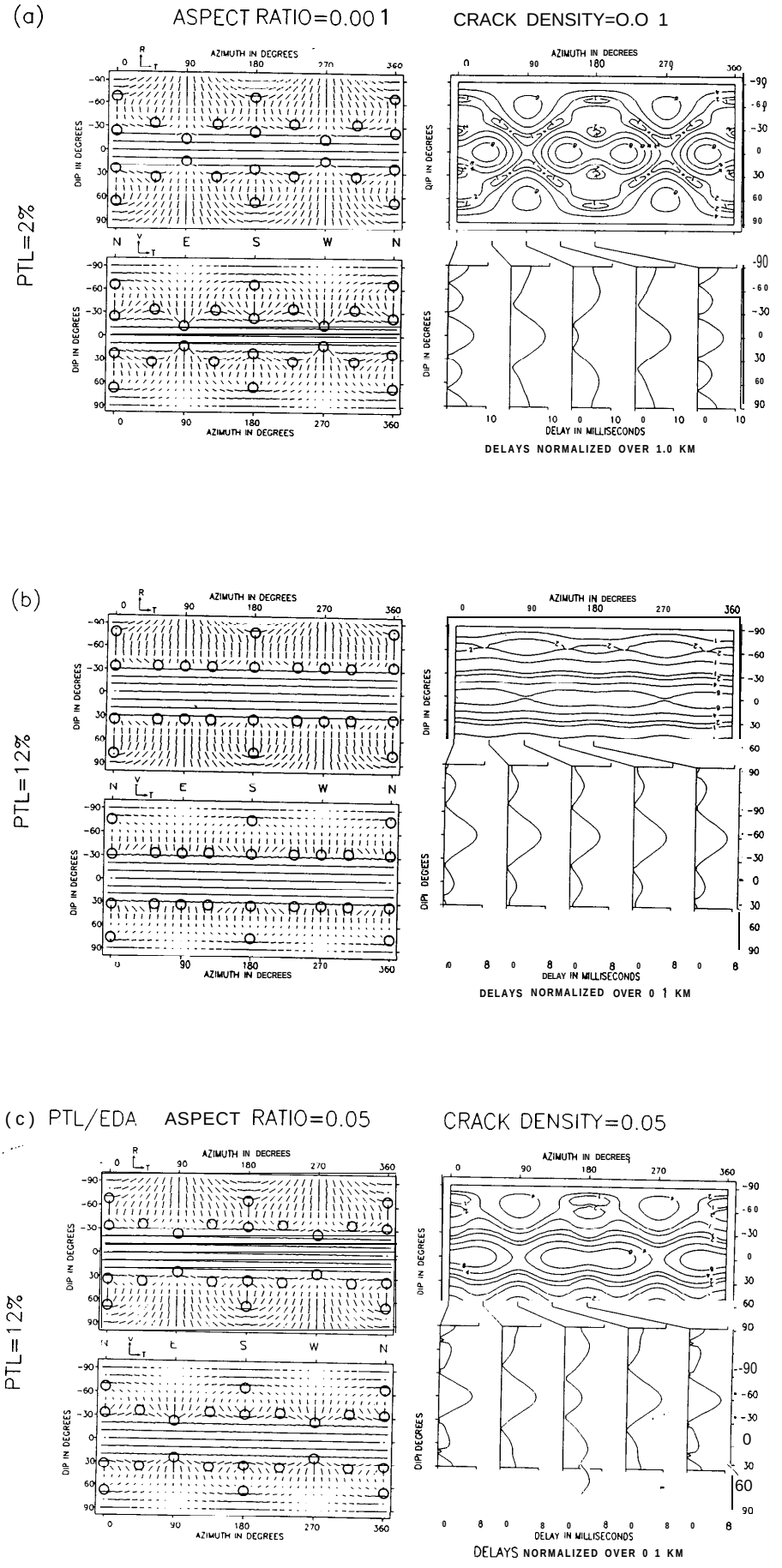

Fig. 2. Plate Carée projections of the polarizations and time delays of split shear waves propagating through CLA anisotropy, for an EDA crack-distribution with crack density ε = 0.01 and aspect ratio y = 0.001 in uncracked matrices with PTL anisotropy: **(a)** PTL1 – 2% differential shear-wave anisotropy; **(b)** PTL2 – 12%; and (c) PTL3 – 22%. Note different normalizations of the contour plots. Format and notation as in Figure 1.

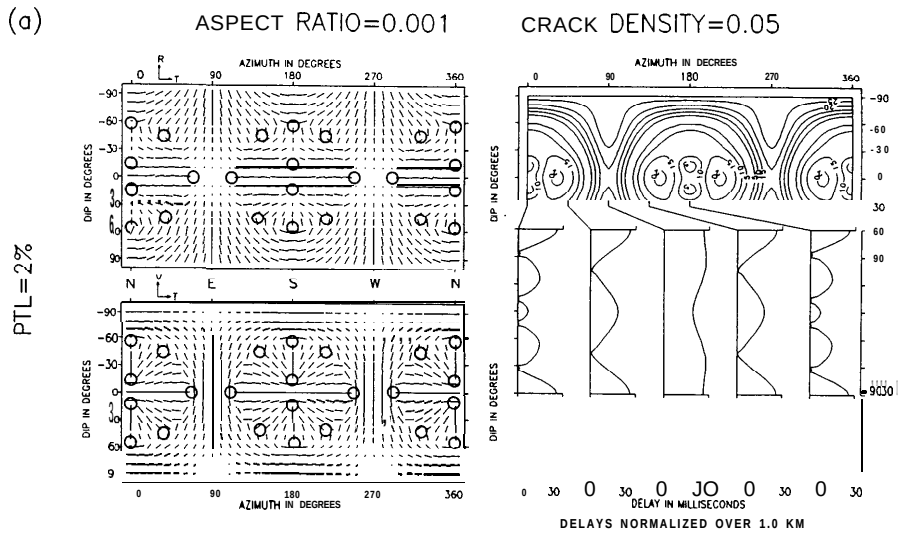

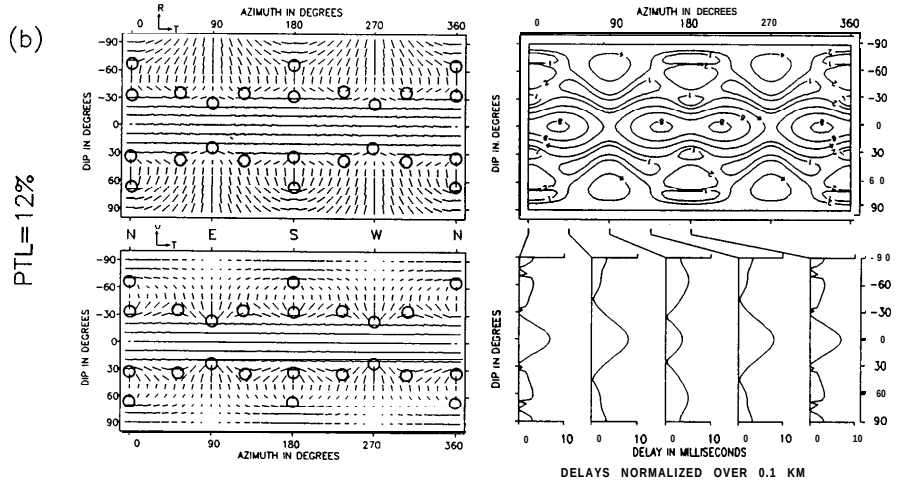

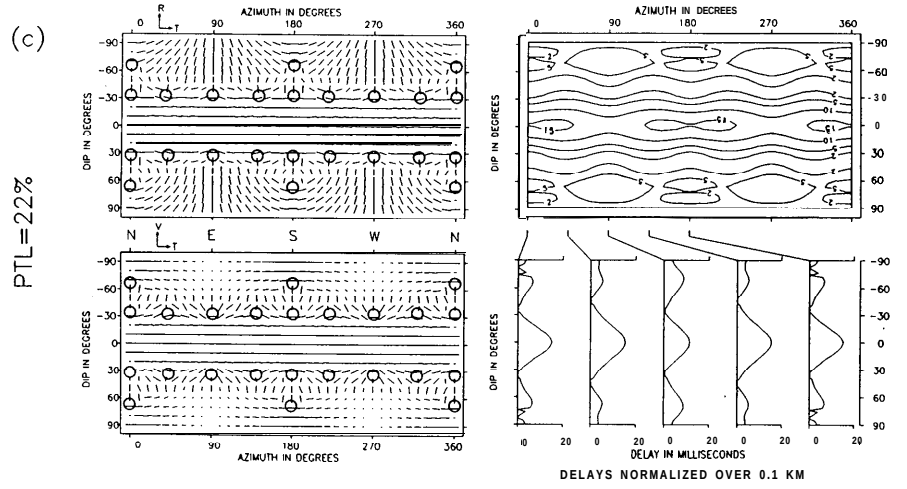

Fig. 3. Similar projections to Figure 2 for EDA crack distributions with crack density $\varepsilon = 0.05$ and aspect ratio $\gamma = 0.001$ in the same three **PTL** anisotropies. Format and notation as in Figure 1.

how shear-wave behaviour may be further used to measure types and relative amounts of anisotropy present in a rock mass. However, observations are needed from a number of azimuths and dips to interpret the polarizations and delays in terms of rock structure. Plate Carée projections may be particularly useful for the interpretation of data sets where the

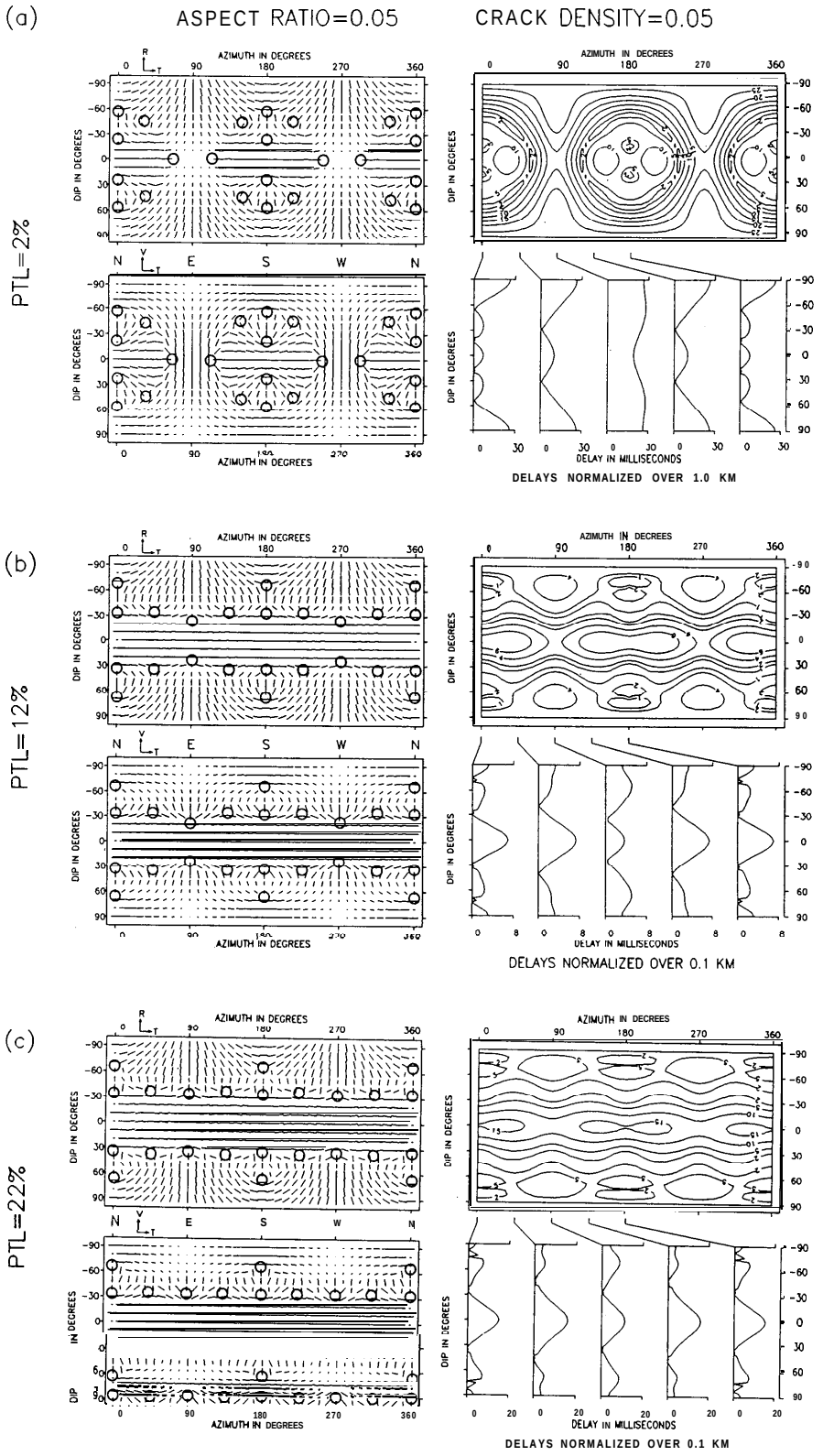

Fig. 4. Similar projections to Figure 2 for EDA crack distributions with crack density ε = 0.05 and aspect ratio y = 0.05 in the same three PTL anisotropies. Format and notation as in Figure 1.

angular coverage is large, as in the experiment described by Holmes et al. (1993) where the results have been plotted in cylindrical projection and interpreted using models similar to the ones used here.

The following conclusions can be drawn from the behaviour of the shear waves for the modelled structures. The polarizations of shear waves at the wide angles typical of CHSs through vertical or near-vertical cracks are no longer parallel to the crack strike in media with orthorhombic symmetry. The point singularities which occur in considerable numbers in combinations of PTL and EDA anisotropies can have a significant effect on shear-wave propagation. The shear-wave polarizations change by 90" near point-singularities and have anomalous time delays between the split shear waves and anomalous amplitudes. These are similar to the findings of Wild and Crampin (199 1).

Furthermore, the directions of the point singularities for the models shown are widely distributed over the range of azimuths and dips. In a CHS it is likely that the directions of propagation would be such that the behaviour of the shear waves would show the effects of propagation near such point-singularities. The accurate positioning of singularities from real data sets and comparison with models are important as the directions (azimuths and angles of incidence) of singularities are critically dependent on the relationships of PTL and EDA anisotropy. These positions may provide a valuable directional correlation with the estimates of PTL and EDA anisotropy which are usually derived from velocity information. This may enable complex field measurements of polarizations and delays to be interpreted in terms of a uniform anisotropic structure, rather than mistaking such features for geological discontinuities.

REFERENCES

Booth, D.C. and Crampin, S., 1985, Shear-wave polarizations on a curved wavefront at an isotropic free-surface: Geophys. J. Roy. Astr. Soc. 83, 3 I - 45.

Bush, I. and Crampin, S., 1987, Observations of EDA and PTL anisotropy in shear-wave VSPs: 57th Ann. Intemat. Mtg., Soc. Expl. Geophys., Exp. Abstr., 646-649.

_____ and _____, 199 1, Paris Basin VSPs: case history establishing combinations of fine-layer (or lithologic) anisotropy and crack anisotropy from modelling shear wavefields near point singularities: Geophys. J. Intemat. **107**, 433-447.

Cliet, C., Brodov, L., Tikonov, A., Marin, D. and Michon, D., 199 I, Anisotropy survey for reservoir delineation: Geophys. J. Intemat. **107**, 417-428.

Crampin, S., 1978, Seismic wave propagation through a cracked solid: polarization as a possible dilatancy diagnostic: Geophys. J. Roy. Astr. Soc. 53, 467-496.

- 9 198 1, A review of wave motion in anisotropic and cracked elastic-media: Wave Motion 3, 343-39 1.

1984, Effective anisotropic elastic constants for wave propagation through cracked solids: Geophys. J. Roy. Astr. Soc. 76, 135-145.

_____, 1985a, Evaluation of anisotropy by shear-wave splitting: Geophysics **50**, 142-152.

_____, 1985b, Evidence of aligned cracks in the Earth's crust: First Break **3**, 3, 12-15.

_____, 1987, Geological and industrial implications of extensive-dilatancy anisotropy: Nature **328**, 49 I-496.

1989, Suggestions for a consistent terminology for seismic anisotropy: Geophys. Prosp. 37, 753-770.

1991, Effects of point singularities on shear-wave propagation in sedimentary basins: Geophys. J. Intemat. **107**, 53 l-543.

_____, 1993a, Arguments for EDA: Can. J. Expl. Geophys. 29, 18-30.

_____, 1993b, A review of the effects of crack geometry on wave propagation through aligned cracks: Can. J. Expl. Geophys. 29, 3-17.

_____ and Lovell, J.H., 1991, A decade of shear-wave splitting in the Earth's crust: what does it mean? what use can we make of it? and what should we do next?: Geophys. J. Intemat. **107**, 387-407.

_____ and Yedlin, M., 1981, Shear wave singularities of wave propagation in anisotropic media: Geophys. J. Roy. Astr. Soc. **49**, 43-46.

Douma, J. and Crampin, S., 1990, The effect of a changing aspect ratio of aligned cracks on shear-wave vertical seismic profiles: a theoretical study: J. Geophys. Res. 95, 11, 293-l 1, 300.

Evans, J.R., 1984, Effects of the free surface on shear wavetrains: Geophys. J. Roy. Astr. Soc. 76, 165-172.

Holmes, G.M., Crampin, S. and Young, R.P., 1993, Preliminary analysis of shear-wave splitting in granite at the Underground Research Laboratory, Manitoba: Can. J. Expl. Geophys. 29, 140- 152.

Hudson, J.A., 1980, Overall properties of a cracked solid: Math. Proc. Cambr. Phil. Soc. **88**, 37 I-384.

_____, 198 1, Wave speeds and attenuation of elastic waves in material containing cracks: Geophys. J. Roy. Astr. Soc. 64, 133- 150.

_____, 1986, A higher order approximation to the wave propagation constants for a cracked solid: Geophys. J. Roy. Astr. Soc. **87**, 265-274.

Kaarsberg, E.A., 1968, Elasticity studies of isotropic and anisotropic rock samples: Trans. Soc. Min. Eng. **241**, 470-475.

Krey, T. and Helbig, K., 1956, A theorem concerning anisotropy of stratified media, and its significance for reflection seismics: Geophys. Prosp. 4, 295-302.

Levin, F.K., 1979, Seismic velocities in transversely isotropic media: Geophysics **44**, 9 18-936.

_____, 1980, Seismic velocities in transversely isotropic media II: Geophysics **45**, 3-17.

Lewis, C., Davis, T.L. and Vuillermoz, C., 1991, Three-dimensional multicomponent imaging of reservoir heterogeneity, Silo Field, Wyoming: Geophysics **56**, 2048-2956.

Li, X.-Y., Mueller, M.C. and Crampin, S., 1993, Case studies of shear-wave splitting in reflection surveys in South Texas: Can. J. Expl. Geophys. 29, 189-215.

Liu, E. and Crampin, S., 1990, Effects of the internal shear-wave window: comparison with anisotropy induced splitting: J. Geophys. Res. 95, 11,275-l 1,281.

_____, _____ and Booth, D.C., 1989, Shear-wave splitting in cross-hole surveys: modeling: Geophysics **54**, 57-65.

_____, _____ and Queen, J.H., 199 1, Fracture detection using cross-hole surveys and reverse vertical seismic profiles at the Conoco Borehole Test Facility, Oklahoma: Geophys. J. Intemat. **107**, 449-463.

Mueller, M.C., 1991, Prediction of lateral variability in vertical fracture intensity using multicomponent shear-wave surface seismic as a precursor to horizontal drilling in the Austin Chalk: Geophys. J. Intemat. **107**, 409-415.

_____, 1992, Using shear waves to predict lateral variability in vertical fracture intensity: The Leading Edge **11**, 2, 29-35.

Postma, G.W., 1955, Wave propagation in a stratified medium: Geophysics **20**, 780-806.

Robertson, J.D. and Corrigan, D., 1983, Radiation patterns of a shear-wave vibrator in near-surface shale: Geophysics 48, 19-26.

Slater, C., Crampin, S., Brodov, L.Y. and Kuznetsov, V.M., 1993, Observations of anisotropic cusps in transversely isotropic clay: Can. J. Expl. Geophys. **29**, 2 16-226.

Wild, P. and Crampin, S., 199 1, The range of effects of azimuthal isotropy and EDA anisotropy in sedimentary basins: Geophys. J. Internat. 107, 5 13-529.

Yardley, G.S. and Crampin, S., 1993, Shear-wave anisotropy in the Austin Chalk, Texas, from multioffset VSP data: case studies: Can. J. Expl. Geophys. 29, 163- 176.